

## Self-similar breakup of near-inviscid liquids

J. R. Castrejón-Pita,<sup>1</sup> A. A. Castrejón-Pita,<sup>1</sup> E. J. Hinch,<sup>2</sup> J. R. Lister,<sup>2</sup> and I. M. Hutchings<sup>1</sup>

<sup>1</sup>*Department of Engineering, University of Cambridge, Cambridge CB3 0FS, United Kingdom*

<sup>2</sup>*Department of Applied Mathematics and Theoretical Physics, University of Cambridge, Cambridge CB3 0WA, United Kingdom*

(Received 22 March 2012; published 5 July 2012)

The final stages of pinchoff and breakup of dripping droplets of near-inviscid Newtonian fluids are studied experimentally for pure water and ethanol. High-speed imaging and image analysis are used to determine the angle and the minimum neck size of the cone-shaped extrema of the ligaments attached to dripping droplets in the final microseconds before pinchoff. The angle is shown to steadily approach the value of  $18.0 \pm 0.4^\circ$ , independently of the initial flow conditions or the type of breakup. The filament thins and necks following a  $\tau^{2/3}$  law in terms of the time remaining until pinchoff, regardless of the initial conditions. The observed behavior confirms theoretical predictions.

DOI: [10.1103/PhysRevE.86.015301](https://doi.org/10.1103/PhysRevE.86.015301)

PACS number(s): 47.55.df, 47.55.db, 47.80.Jk

Drop formation by jet breakup and pinchoff is a process involved in almost any scenario where a liquid is delivered by jetting or dripping and fluid surfaces are broken. Industrial examples of these events occur in inkjet printing, spray deposition and painting, and the dispensing of liquids by pipetting [1]. In addition, there are biological instances in which liquid jets and droplets are formed, as in the attack mechanism of the archerfish [2]. In all these cases, an initially continuous jet is eventually broken up into drops by surface tension forces. Studies of pinchoff and breakup of liquids are not theoretically simple due to finite-time singularities and the disparity between dimensional and time scales found in the Navier-Stokes equation describing the dynamics [3,4]. Experiments in this area are challenging, as they are required to resolve features at very small length scales and record events at high speed for long periods of time in order to capture the fluid behavior during the different time scales involved in breakup [3]. Regardless of these complications, important advances have been achieved in the study of drop formation and breakup. Theoretical and experimental models for Newtonian liquids have confirmed that the filament aspect ratio and the Ohnesorge number  $Oh$  determine whether a discrete filament condenses lengthwise into a droplet or breaks up into satellite droplets, where  $Oh = \mu/\sqrt{\rho R_0 \sigma}$ ,  $R_0$  is the initial radius of the filament,  $\mu$  is the viscosity,  $\rho$  is the density, and  $\sigma$  is the surface tension of the liquid [5–7]. Previous research has demonstrated that the length scale of the pinchoff region of thinning viscous fluids obeys a  $\sim \tau Oh^{-1}$  scaling, where  $\tau$  is the time remaining until breakup [3,4]. Using numerical methods, it has been found that (i) in the pinchoff of inviscid fluids under the action of surface tension the thinning (neck contraction) follows a scaling law  $\sim \tau^{2/3}$ , (ii) the fluid surface of the droplet overturns before the breakup, and (iii) the shape of the breakup region is self-similar and thus independent of initial conditions [3,8,9]. By relying on the condition of self-similarity, experimental studies with near-inviscid liquids have demonstrated that this scaling law is followed down to the nanometer and nanosecond scales [10,11]. Another important conclusion as described in Ref. [8] is that, regardless of the initial shape of a pendant liquid drop, the included angle at the tip of the conical-shaped filament at breakup is  $\sim 18.1^\circ$ . Although this theoretically predicted value of the breakup

angle has been used to prove the neck-thinning scaling law in some studies [11], an experimental corroboration of the correctness of this value has, however, remained untested. The experimental validation of some aspects of these scaling laws has provided a reliable standard against which to test numerical algorithms that model the formation of droplets by dripping and jetting [3,9]. However, given that these simulations usually contain several free parameters, other standards are desirable for further parametric validations, including the breakup angle.

In this Rapid Communication the breakup angle and the thinning neck diameter of two near-inviscid liquids are studied under different flow conditions by high-speed imaging and image analysis. The results demonstrate that the geometry of pinchoff is self-similar, the necking scaling law is universal, and the surface breakup angle prior to breakup is consistent with the predicted value of  $18.1^\circ$ .

For a liquid dripping from a tube at low  $Oh$ , breakup can occur at various locations. These are identified as A, B, and C in Fig. 1. In region A, front pinching produces the first point of breakup leading to the formation of a main droplet and a filament. In region B, further pinchoff detaches the ligament of liquid from the remaining fluid in the nozzle, forming the so-called satellite filament. In region C, this filament undergoes further breakups, forming secondary satellite droplets. In our experiments we acquired high- (temporal and spatial) resolution images of these different regions by high-speed imaging in a shadowgraph configuration for different flow rates. Image analysis was applied to obtain the breakup angle and the minimum neck diameter. Examples of images for front pinching (region A) are shown in Fig. 2 and examples of the breakup within the filament (region C) are presented in Fig. 3.

The shadowgraph setup consisted of a 150-W fiber optics lamp (MFO-90, Microtec), an optical diffuser (25.4-mm circular engineered microlens array, RPC Photonics), and a high-speed camera (Phantom V310, Vision Research) coupled to a microscope lens (12 $\times$  ultra zoom, Navitar). Although this optical system is known to produce pincushion distortion at the edges of large CCD sensors [12], the effect is negligible here as only a small central fraction of the sensor is used. This distortion was tested by the imaging of a precision square grid (microscope graticule) at the appropriate frame speeds. The lens-camera configuration gave a fixed resolution of

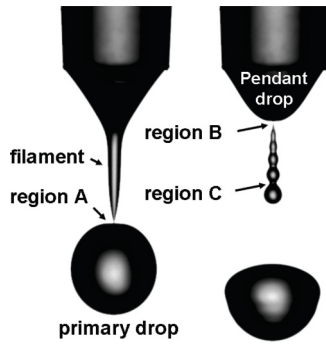


FIG. 1. Breakup regions found in dripping. The breakup at region A forms the primary drop, the breakup in region B detaches the filament from the pendant drop, and region C is found at one or several points of breakup within the filament.

$193 \pm 1$  pixels/mm. During the experiments three frame rates were used: 220 000 frames/s with an exposure time of  $1.93 \mu\text{s}$  and a field of view of  $128 \times 64$  pixels<sup>2</sup>, 78 200 frames/s with an exposure time of  $2.02 \mu\text{s}$  and a field of view of  $256 \times 128$  pixels<sup>2</sup>, and 23 000 frames/s with an exposure time of  $2.02 \mu\text{s}$  and a field of view of  $512 \times 256$  pixels<sup>2</sup>. Given the finite frame speed and exposure times of the imaging system, the true time of breakup  $t$  could be

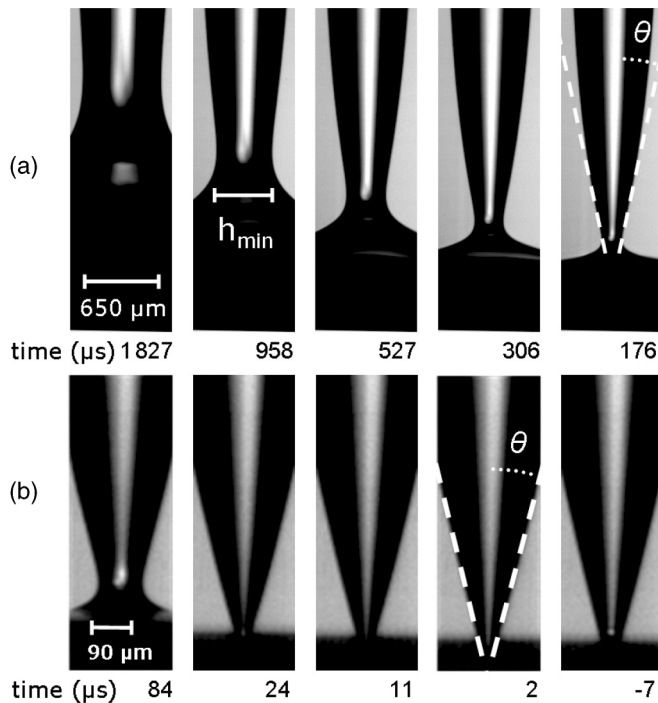


FIG. 2. Imaging of the pinchoff process in region A for a dripping water droplet; the time shown corresponds to the time to breakup. For the conditions observed, the flow is  $Q_1^{\text{water}} = 0.092 \text{ ml s}^{-1}$ . The videos from which these images were extracted were recorded at two camera speeds: The frame rate was (a)  $23 \times 10^3$  frames/s and (b)  $220 \times 10^3$  frames/s. Image analysis was used to extract the angle of the conical filament  $\theta$  from which the droplet is breaking up. Two microseconds prior to breakup ( $t = 2 \mu\text{s}$ ),  $\theta = 16.9 \pm 0.2^\circ$  degrees; the asymptotic analysis shows that at the point of breakup ( $t = 0 \mu\text{s}$ )  $\theta = 17.9 \pm 0.2^\circ$ .

TABLE I. Experimental conditions.

Flow rate	$Q \times 10^7 / \text{m}^3 \text{s}^{-1}$	$We \times 10^3$	$Oh \times 10^3$
$Q_1^{\text{water}}$	$0.92 \pm 0.01$	$0.54 \pm 0.03$	$2.22 \pm 0.11$
$Q_2^{\text{water}}$	$2.50 \pm 0.01$	$4.01 \pm 0.22$	$2.22 \pm 0.11$
$Q_3^{\text{water}}$	$4.96 \pm 0.01$	$16.03 \pm 0.87$	$2.22 \pm 0.11$
$Q_4^{\text{water}}$	$7.5 \pm 0.01$	$36.06 \pm 0.20$	$2.22 \pm 0.11$
$Q_1^{\text{ethanol}}$	$2.36 \pm 0.01$	$8.60 \pm 0.51$	$7.64 \pm 0.25$

determined only to a precision of one-half of the interframe time (2.3, 6.4 and  $21.7 \mu\text{s}$ ). In these experiments, the exact breakup time is located between those consecutive images showing a connected surface and the evidence of breakup (usually highlighted by the appearance of the bulbous end formed during the contraction of the filament as seen in the final image of Fig. 2(b)).

Dripping was produced by pumping the liquid from a reservoir to a 12-mm-long conical plastic (polymethylpentene) nozzle with a measured inlet angle of  $4.5^\circ$  and outlet diameter of 5.6 mm. A sealed and partly filled liquid container was placed between the pump (Premotec BL58) and the nozzle in order to damp out any irregularity in the pressure and to remove any air bubbles from the liquid; a similar system has been previously used to produce continuous jets [13]. The droplets dripped into the reservoir and the liquid was recirculated by the pump. The working fluids consisted of tridistilled water ( $\mu = 1.00 \pm 0.05 \text{ mPa s}$ ,  $\rho = 998 \pm 5 \text{ kg m}^{-3}$ , and  $\sigma = 72.1 \pm 0.1 \text{ mN m}^{-1}$ ) and ethanol ( $\mu = 1.7 \pm 0.1 \text{ mPa s}$ ,  $\rho = 789 \pm 5 \text{ kg m}^{-3}$ , and  $\sigma = 22.4 \pm 0.1 \text{ mN m}^{-1}$ ) and the experiments were carried out at  $21^\circ\text{C}$ . Fluid density, viscosity, and surface tension were measured with an Anton Paar DMA 35N density meter, a Hidramotion 700 Viscolite viscometer,

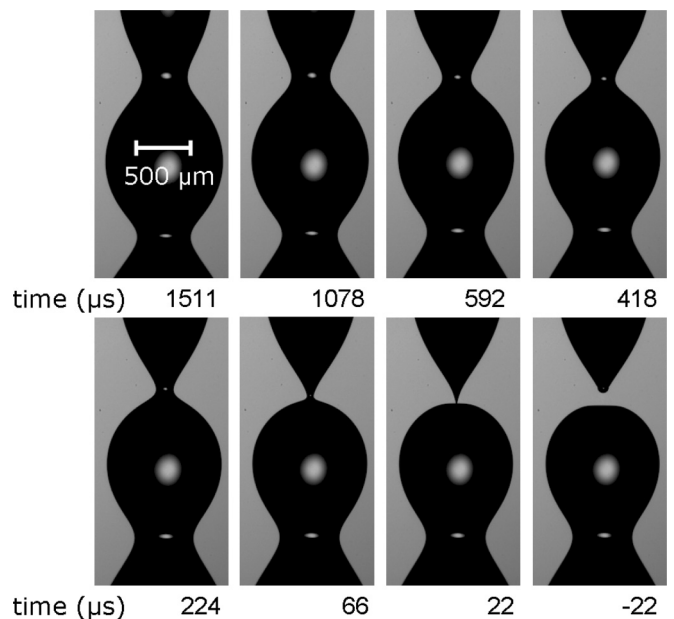


FIG. 3. Imaging of the pinchoff process in region C (filament breakup). The frame rate used in this experiment was  $23 \times 10^3$  frames/s. For the condition observed, the flow is  $Q_4^{\text{water}} = 0.750 \text{ ml s}^{-1}$ .

and a SITA bubble pressure t-15 tensiometer (at a bubble lifetime of 500 ms), respectively.

Four different flow rates  $Q$  were studied for water and one flow rate for ethanol, as listed in Table I. The flow rates for experiments with water were chosen to limit the Ohnesorge Oh and Weber We numbers to that of simple dripping [14] (where  $We = \rho Q^2 / \pi^2 \sigma R^3$  and  $R$  is the nozzle radius). Smaller flow rates were limited by the particular characteristics of the fluid pump and the configuration used in this work. Breakup within the filament (region C) was observed only for water at the two highest flows ( $Q_3^{\text{water}}$  and  $Q_4^{\text{water}}$ ). For lower flow rates the filament did not break up but contracted into a single satellite droplet or recombined with the pendant droplet producing no satellites.

The boundary of inviscid liquid surfaces collapsing just before the pinchoff has been described as similar to that of a double cone [8], the region near the stalk of an apple [10], or a cone piercing a plate [11]. This geometrical shape is obtained by the overturning of the liquid surface prior to breakup. This overturning is not visible in Figs. 2 and 3 as these images are taken perpendicular to the direction of jetting and the pinchoff region is therefore obscured by the fluid between it and the camera. This effect limits the observation of the necking process and the measurement of  $h_{\min}$  [3]. Images were analyzed to determine the minimum visible neck and the small angle of pinchoff  $\theta$  at various times. This process was carried out in MATLAB by superimposing straight lines on to the fluid boundaries on the small angle side from  $h = h_{\min}$  to  $4h_{\min}$ . The small pinchoff angle is therefore half the angle between these linear fits. Although the surface overturning prevented the direct measurement of the angle at the point of minimum neck width, the angle was measured on the surface directly

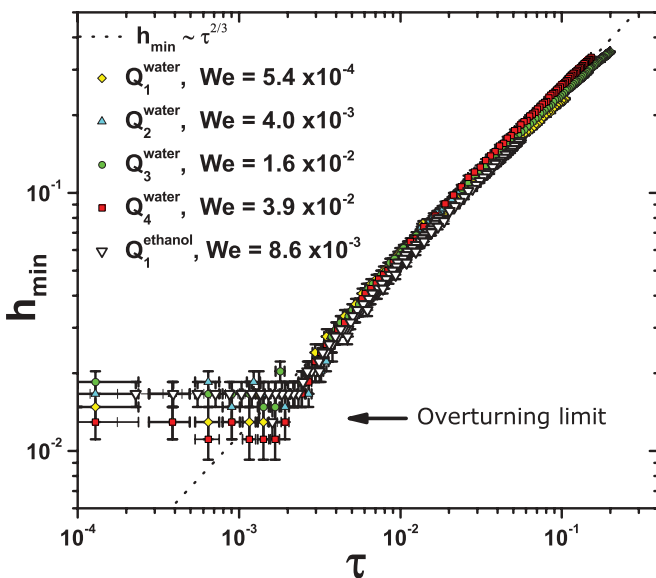


FIG. 4. (Color online) Experimental measurements of the minimum neck diameter  $h_{\min}$  in terms of the dimensionless time  $\tau$  to breakup for different fluids and different flows. Regardless of the condition of flow, within simple dripping the thinning follows a self-similar behavior. The dotted line represents the potential flow scaling law. The measurement of  $h_{\min}$  is limited by the overturning of the droplet surface.

before the overturning point. Shadowgraphy was particularly useful for this analysis as it produces images with very high contrast, which consequently reduces the experimental error. Results are shown in Figs. 4 and 5.

The effects of gravity are considered unimportant for flows on shorter scales than the gravitational capillary length  $l_G = \sqrt{2\sigma/\rho g}$  and are negligible near the breakup [15]. Under these experimental conditions,  $l_G^{\text{water}} = 3.8$  mm and  $l_G^{\text{ethanol}} = 2.4$  mm. Given that the field of view of our imaging system was smaller than these values, the effects of gravity on the experimental results presented in this Rapid Communication can be ignored. The viscous drag of the surrounding air becomes important for neck diameters smaller than  $\sim R(\mu_{\text{air}}\text{Oh}^2/\mu)$ , where  $\mu_{\text{air}}$  is the air viscosity [16]. This value is  $\sim 0.3$  nm for water and  $\sim 1.7$  nm for ethanol, which are orders of magnitude smaller than the length scales studied here. Aerodynamic and inertial effects influence the breakup process when the gas Weber number  $We_g > 0.2$ , where  $We_g = (\rho_g/\rho)We$  and  $\rho_g$  is the density of air [17]. In this work,  $We_g^{\text{water}}$  ranges from  $6.5 \times 10^{-7}$  to  $4.5 \times 10^{-5}$  and  $We_g^{\text{ethanol}} = 1.3 \times 10^{-5}$ . Consequently, these effects are also considered negligible.

The first set of results, shown in Fig. 4, have been put in dimensionless form by using the nozzle radius and the capillary time  $t_c = \sqrt{\rho R^3/\sigma}$ , so that  $\tau = t/t_c$ . Figure 4 shows that the neck thinning near the breakup is consistent with the scaling law  $h_{\min} \sim \tau^{2/3}$  regardless of the flow initial conditions or the liquid properties. The observed overturning limit is also consistent with previous experimental and numerical results obtained for a different (single) flow [3].

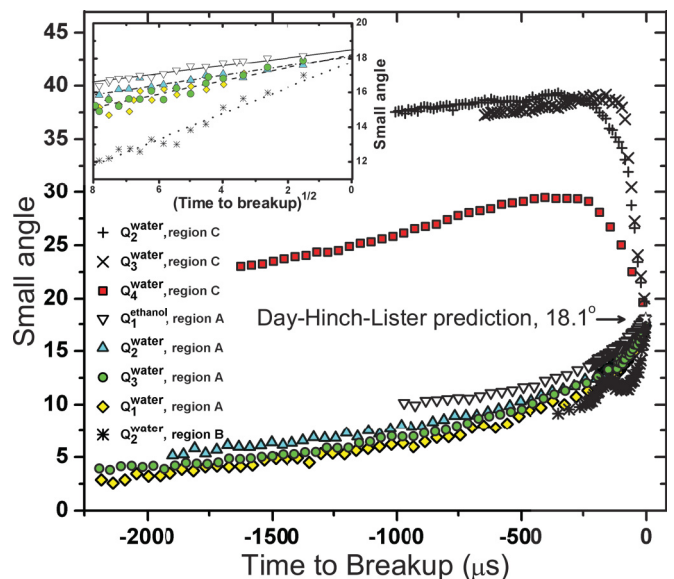


FIG. 5. (Color online) Small pinchoff angle for different flow conditions, breakup regions, and fluids. The mean of the convergent angle value for all the cases is  $\theta = 18.0 \pm 0.4^\circ$ . According to the theory in Ref. [18], approaching pinchoff, all solutions tend towards self-similarity with the same limiting exponent: This exponent appears both numerically and experimentally (see the inset) to be about 0.5. The angles do not approach the asymptotic value of  $18.1^\circ$  along the same curve because the path depends on the initial conditions.

Self-similarity is a geometrical property that in liquids can be assessed by analyzing surface shapes. Figure 5 shows the evolution of the small angle in terms of the time to breakup for different flow conditions, different regions of breakup, and different fluids. For the experiments in region A the small angle slowly evolves from very small angles (as the filament is initially almost cylindrical) with a rapid increase during the final few microseconds before the breakup. In region B the satellite filament undergoes further deformation and multiple breakups that generate secondary satellite droplets. This interesting dynamics shows an alternate route to breakup as there is no preexisting filament from where a main drop can pinch off, but the process starts with two (or more) bulbous regions of fluid, separated by a contracting neck. The angle is therefore affected greatly by the rapid neck contraction and follows a different path: It evolves from large values to a maximum for several hundreds of microseconds and then decays rapidly, reaching the much smaller angle during the final tens of microseconds prior to breakup. These rather different dynamics permit the study of breakup from two different approaching directions (from angles greater than  $18.1^\circ$  and less than  $18.1^\circ$ ). Region C presents somewhat different dynamics, as it is affected by the primary breakup (the detachment of the main droplet). As soon as the main droplet breaks from the filament, the latter rapidly contracts and excites capillary waves that travel all the way up to the contracting neck where the filament detaches from the fluid in the nozzle (breakup region B). This generates an oscillatory effect in the

evolution of the small angle. This is clearly observed in the data plotted in Fig. 5. It is also important to note that during the final moments before breakup, however, such oscillation is no longer evident and the small angle follows a similar behavior to that of region A.

As can be observed in Fig. 5, all the experimental data asymptotically approach a common angle at breakup. Following Ref. [8], the asymptotic value was calculated by plotting the small angle as a function of  $\tau^{1/2}$ , giving an adequately straight line for the last 80  $\mu\text{s}$  before breakup; the final cone angle was deduced by extrapolation from these linear fits. In all the cases explored in this work the extrapolated angle was never outside the confidence interval of  $2\sigma_s$  from the theoretical value of  $18.1^\circ$  (where  $\sigma_s$  is the experimental error). It is remarkable that regardless of the flow, which effectively controls the initial shape of the fluid, the final angle of breakup approaches the same asymptotic value, i.e., the breakup is self-similar. In summary, the results presented in this Rapid Communication show that the geometry of the breakup of near-inviscid fluids is self-similar in the domain of simple dripping. It has also been shown that, independently of initial conditions and fluid characteristics, the necking of the liquid scales with  $\tau^{2/3}$  and asymptotically approaches a unique angle of  $18.0 \pm 0.4^\circ$ .

This project was supported by the United Kingdom Engineering and Physical Sciences Research Council through the GlassJet and I4T projects (Grants No. EP/G029458/1 and No. EP/H018913/1).

- 
- [1] O. A. Basaran, *AIChE J.* **48**, 1842 (2002).
  - [2] T. Schlegel, C. J. Schmid, and S. Schuster, *Curr. Biol.* **16**, R836 (2006).
  - [3] A. U. Chen, P. K. Notz, and O. A. Basaran, *Phys. Rev. Lett.* **88**, 174501 (2002).
  - [4] J. Eggers, *Phys. Rev. Lett.* **71**, 3458 (1993).
  - [5] R. M. S. M. Schulkes, *J. Fluid Mech.* **309**, 277 (1996).
  - [6] P. K. Notz and O. A. Basaran, *J. Fluid Mech.* **512**, 223 (2004).
  - [7] A. A. Castrejón-Pita, J. R. Castrejón-Pita, and I. M. Hutchings, *Phys. Rev. Lett.* **108**, 074506 (2012).
  - [8] R. F. Day, E. J. Hinch, and J. R. Lister, *Phys. Rev. Lett.* **80**, 704 (1998).
  - [9] J. R. Castrejón-Pita, N. F. Morrison, O. G. Harlen, G. D. Martin, and I. M. Hutchings, *Phys. Rev. E* **83**, 036306 (2011).
  - [10] J. C. Burton, J. E. Rutledge, and P. Taborek, *Phys. Rev. Lett.* **92**, 244505 (2004).
  - [11] J. C. Burton, J. E. Rutledge, and P. Taborek, *Phys. Rev. E* **75**, 036311 (2007).
  - [12] J. R. Castrejón-Pita, G. D. Martin, and I. M. Hutchings, *J. Imaging Sci. Technol.* **55**, 040305 (2011).
  - [13] J. R. Castrejón-Pita, N. F. Morrison, O. G. Harlen, G. D. Martin, and I. M. Hutchings, *Phys. Rev. E* **83**, 016301 (2011).
  - [14] B. Ambravaneswaran, H. J. Subramani, S. D. Phillips, and O. A. Basaran, *Phys. Rev. Lett.* **93**, 034501 (2004).
  - [15] A. U. Chen and O. A. Basaran, *Phys. Fluids* **14**, L1 (2002).
  - [16] J. R. Lister and H. A. Stone, *Phys. Fluids* **10**, 2758 (1998).
  - [17] W. Hove *et al.*, *Phys. Fluids* **22**, 122003 (2010).
  - [18] D. Leppinen and J. R. Lister, *Phys. Fluids* **15**, 5683 (2003).